

The adsorption of acetic acid on Au/Pd(111) alloy surfaces

Z. Li, F. Calaza, F. Gao, W.T. Tysoe *

Department of Chemistry and Laboratory for Surface Studies, University of Wisconsin-Milwaukee, Milwaukee, WI 53211, USA

Received 30 October 2006; accepted for publication 26 December 2006

Available online 3 January 2007

Abstract

The adsorption of acetic acid is studied as a function of gold content by temperature-programmed desorption and reflection–absorption infrared spectroscopy on Au/Pd(111) alloys formed by depositing 5 ML of gold onto a Pd(111) surface and heating to various temperatures. For mole fractions of gold greater than ~ 0.5 , acetic acid adsorbs molecularly and desorbs intact with an activation energy of ~ 52 kJ/mol. This acetic acid is present as catemers, where the nature of the catemer is found to depend on gold concentration. When the relative gold concentration is less than ~ 0.33 , adsorption of acetic acid at 80 K and heating to ~ 207 K forms η^1 -acetate species on the surface. On further heating, these can either thermally decompose to eventually evolve hydrogen, water and oxides of carbon, or form η^2 -acetate species, where the coverage of reactively formed η^2 -acetate species increases with decreasing gold concentration in the near surface region.

© 2006 Elsevier B.V. All rights reserved.

Keywords: Infrared absorption spectroscopy; Chemisorption; Palladium–gold alloy; Acetic acid

1. Introduction

Acetic acid adsorbs molecularly on Pd(111) surfaces at low temperatures, forming η^2 -acetate species on heating to ~ 300 K, although some evidence has been presented for the formation of η^1 -species [1]. The η^2 -acetate species adsorbs with the C–COO plane oriented perpendicularly to the Pd(111) surface with the acetate oxygen atoms located approximately above palladium atop sites [2]. Density functional theory calculations have demonstrated that the acetate species thermally decompose (at ~ 400 K) by the C–COO plane tilting such that the methyl group can interact with the surface leading to C–H bond cleavage [3,4] and the kinetics of this decomposition pathway have been shown to occur “explosively”, that is with extremely fast kinetics, on carbon-covered Pd(110) [5] and oxygen-covered Pd(111) [6]. Palladium catalyzes the synthesis of vinyl acetate monomer (VAM) from ethylene, acetic acid and

oxygen and the reaction on Pd(111) has been shown to proceed via a pathway first proposed by Samanos et al. [7] in which ethylene reacts with adsorbed acetate species to form an acetoxyethyl–palladium intermediate, which yields VAM via a β -hydride elimination reaction [8]. Total combustion of acetic acid and ethylene can also occur so that the selectivity to VAM when catalyzed by palladium alone is $\sim 85\%$. Clearly improving the reaction selectivity will have significant economic benefits, as well a decreasing the total exothermicity of the reaction thus mitigating problems associated with handling the heat load in a commercial reactor. This is accomplished by alloying the palladium with gold, leading to a significant improvement in selectivity to approximately 92% [9]. While this selectivity is impressively high, there is evidently still room for improvement. In order to understand the effects of alloy formation on the surface chemistry of acetic acid, the following work explores the chemistry of acetic acid on gold–palladium (111) alloy surfaces using a combination of reflection–absorption infrared spectroscopy (RAIRS) and temperature-programmed desorption (TPD). The alloys are obtained by adsorbing ~ 5 ML of gold onto a

* Corresponding author. Tel.: +1 414 229 5222; fax: +1 414 229 5036.
E-mail address: wtt@uwm.edu (W.T. Tysoe).

clean Pd(111) surface at room temperature and by annealing to various temperatures to cause gold to diffuse into the palladium substrate. This approach provides a particularly convenient method for studying the effects of alloying since it allows a relatively large numbers of alloy compositions to be compared. Since Au/Pd(111) exhibits no additional ordered low-energy electron diffraction (LEED) features, except for the substrate (1×1) spots, it has been suggested that the gold and palladium atoms are randomly distributed at the surface thereby potentially allowing correlations to be made between various surface Au–Pd ensembles and their chemical properties [10].

2. Experimental

The equipment used to collect RAIRS and TPD data has been described in detail elsewhere [11]. Briefly RAIRS data are collected with a Bruker Equinox spectrometer, typically for 1000 scans at a resolution of 4 cm^{-1} . TPD data were collected in another chamber that was equipped with a Dychor quadrupole mass spectrometer interfaced to a computer that allowed up to five masses to be sequentially monitored in a single experiment. The sample could be cooled to 80 K in both chambers by thermal contact to a liquid-nitrogen-filled reservoir and resistively heated to $\sim 1200 \text{ K}$.

The Pd(111) single crystal was cleaned using a standard procedure and its cleanliness monitored using Auger spectroscopy and temperature-programmed desorption collected following oxygen adsorption [12]. Gold was evaporated from a small alumina tube furnace [13], which enabled controlled and reproducible evaporation rates to be achieved. In order to precisely control the temperature of the gold, and therefore its evaporation rate, a C-type thermocouple was placed into the gold pellet. The amount of gold deposited onto the surface was monitored using Auger spectroscopy from the peak-to-peak intensities of the Au NVV and Pd MNN Auger features and the monolayer coverage was gauged from breaks in the gold uptake signal. The gold palladium alloy was formed according to a recipe developed by Lambert and co-workers [10] by initially adsorbing 5 ML of gold then by annealing to various temperatures for a period of five minutes in ultrahigh vacuum to produce the desired Au/Pd atomic ratio. The sample was then allowed to cool, following which acetic acid was adsorbed onto the surface. The resulting variation in Auger peak-to-peak intensity with annealing temperature was in excellent agreement with previous work [10] and gold concentrations are quoted based on this calibration. This gold concentration in the alloy, measured from the relative Auger peak-to-peak intensities corresponded well to the lattice spacings of the surface measured by LEED compared with those for the corresponding bulk alloys. It should be emphasized that such electron-based techniques probe not only the outermost layers, but also several layers into the bulk and yield the average composition of these layers. Since the surface free energy of gold is lower than

that of palladium [14,15], the outermost layer is likely to be significantly enriched with gold compared to the bulk. Such an enrichment has been found experimentally for gold–palladium alloys formed on a Mo(110) substrate [16]. Thus, the gold or palladium compositions quoted in the following reflect their mole fractions in the near surface region, not necessarily directly on the surface.

The glacial acetic acid (Aldrich, 99.99+% purity) was transferred to a glass bottle which was attached to a gas-handling line for introduction into the vacuum chamber and was further purified by several freeze–pump–thaw cycles. Its purity was confirmed by mass spectroscopy.

3. Results

Temperature-programmed desorption (TPD) experiments of acetic acid adsorbed on clean Pd(111) at 170 K reveal acetic acid desorption at ~ 230 and $\sim 310 \text{ K}$, with major decomposition products consisting of CO_2 (200–400 K), CO (490 K) and hydrogen ($\sim 380 \text{ K}$) and water over the same temperature range [1]. These desorption processes have been modeled theoretically where they have been assigned to the presence of an η^2 -acetate species on the surface that decomposes by rocking about the OCO group until the methyl group can reach the surface and dehydrogenate [2]. In order to focus on the essentials of the desorption and reaction pathways of acetic acid on surfaces with a wide range of alloy compositions, TPD spectra will be displayed for a saturated overlayer of acetic acid (just prior to the onset of multilayer desorption) focusing on the desorption of acetic acid (60 amu), CO_2 (44 amu), carbon monoxide (28 amu) and hydrogen (2 amu). Fig. 1

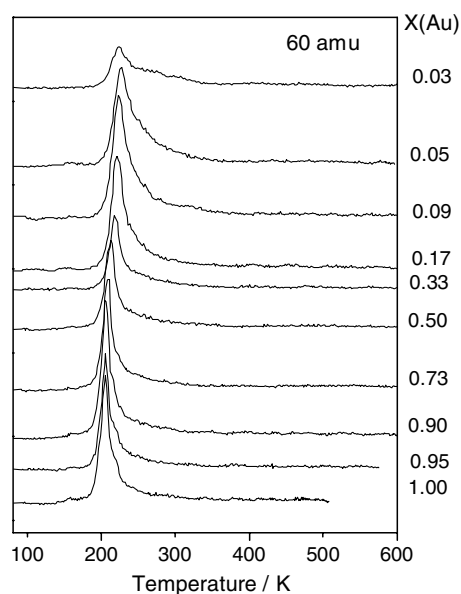


Fig. 1. TPD spectra collected monitoring 60 amu (acetic acid) following adsorption of acetic acid (1.2 L) on various Au/Pd(111) alloys at 80 K using a heating rate of 3.7 K/s. The mole fraction of gold in each alloy is indicated adjacent to the corresponding spectrum.

displays the acetic acid (60 amu) TPD spectra as a function of gold composition in the near surface region. Gold mole fractions are displayed adjacent to the corresponding desorption spectrum and are estimated from the intensity ratios of the gold NVV Auger features compared to the palladium MNN Auger features and converted into gold concentration using the calibration curves from Refs. [10,17]. The spectra show a very slight increase in peak desorption temperature as the gold concentration decreases to ~ 0.73 , where the peak desorption temperature is ~ 201 – 205 K corresponding to a desorption activation energy of ~ 52 kJ/mol where this value is estimated using the Red-head method [18], assuming a pre-exponential factor of $1 \times 10^{-13} \text{ s}^{-1}$. The peak temperature increases slightly more rapidly with decreasing gold concentration for gold concentrations of ~ 0.5 and lower. This is accompanied by a broadening of the TPD features and the appearance of a higher-temperature tail. There are no drastic changes in acetic acid desorption yield over almost the whole gold concentration range except for the lowest gold concentration (~ 0.03), where the acetic acid desorption feature attenuates drastically, exhibiting additional weak but identifiable features at ~ 230 , 260 and 310 K, similar to those found on clean Pd(111) [1]. The corresponding 44 amu spectra are displayed in Fig. 2, where the peak at ~ 200 K is due to a fragment of the desorbing acetic acid and shows the same trend in peak temperature and intensity as seen in Fig. 1. The remainder of the features are assigned to CO_2 desorption due to the surface-induced decomposition of acetic acid. This reveals that there is essentially no CO_2 evolution for gold concentrations greater than ~ 0.5 while, for lower gold concentrations, the CO_2

yield increases with decreasing gold concentration, with a desorption peak temperature that shifts from ~ 550 K for a gold concentration of ~ 0.33 , to ~ 430 K when the surface region contains only 3% gold and resembles, but is not completely identical to, the desorption profile from clean Pd(111) [1]. The corresponding 2 amu (hydrogen) desorption profiles are displayed in Fig. 3, where a similar trend in reactivity is found. In this case, the 2 amu fragment of acetic acid, giving rise to the weak ~ 210 K feature, is very small. Again, no hydrogen is found to desorb for gold mole fractions larger than ~ 0.5 and the amount of hydrogen that desorbs from the surface increases rapidly as the gold concentration decreases. Hydrogen desorbs in two states, one at ~ 270 K for gold mole fractions between 0.33 and 0.09, which increases in temperature to ~ 350 K for a gold concentration of ~ 0.03 , and a higher-temperature state appears between 440 and 480 K, depending on gold concentration. The corresponding 28 amu (carbon monoxide) desorption spectra are displayed in Fig. 4. Again, the feature at ~ 210 K is due to mass spectrometer ionizer fragmentation of desorbing acetic acid. In this case, some CO desorption is detected for gold concentrations greater than ~ 0.5 , which may indicate some acetic acid decomposition but may also be due to some background CO adsorption. Nevertheless, the CO desorption yield increases with decreasing gold concentration in accord with the 44 (CO_2) and 2 (H_2) amu desorption profiles (Figs. 2 and 3).

Reflection–absorption infrared spectra (RAIRS) were collected for a saturated overlayer (1.2 L exposure) of acetic acid adsorbed on various gold alloy surfaces as a function of annealing temperature. Again, the spectra are compared for various alloy surfaces following adsorption

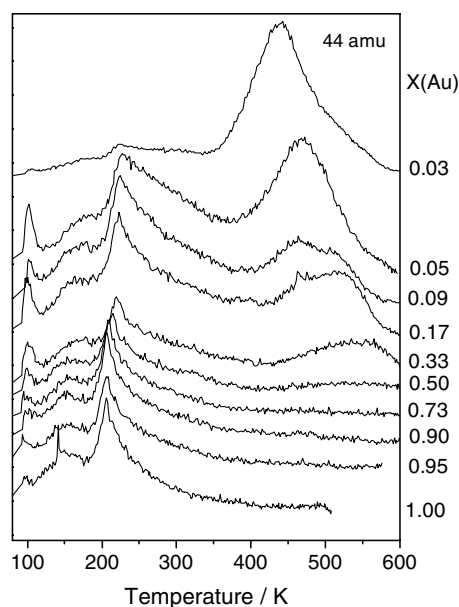


Fig. 2. TPD spectra collected monitoring 44 amu (carbon dioxide) following adsorption of acetic acid (1.2 L) on various Au/Pd(111) alloys at 80 K using a heating rate of 3.7 K/s. The mole fraction of gold in each alloy is indicated adjacent to the corresponding spectrum.

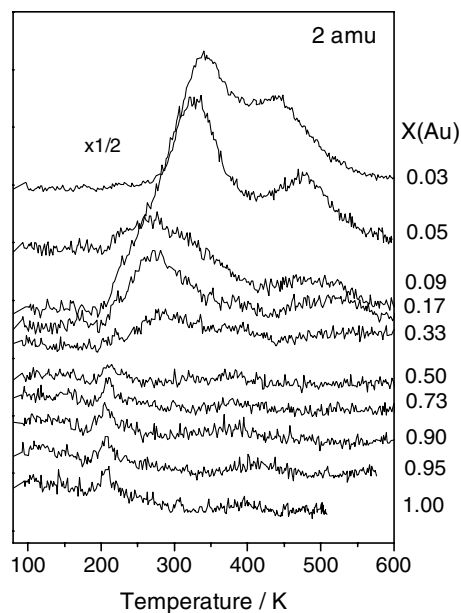


Fig. 3. TPD spectra collected monitoring 2 amu (hydrogen) following adsorption of acetic acid (1.2 L) on various Au/Pd(111) alloys at 80 K using a heating rate of 3.7 K/s. The mole fraction of gold in each alloy is indicated adjacent to the corresponding spectrum.

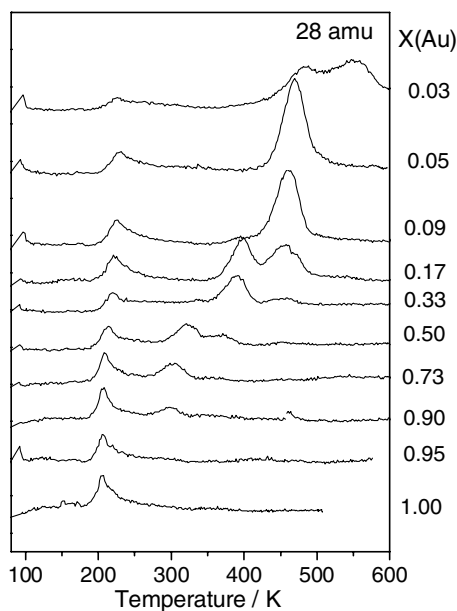


Fig. 4. TPD spectra collected monitoring 28 amu (carbon monoxide) following adsorption of acetic acid (1.2 L) on various Au/Pd(111) alloys at 80 K using a heating rate of 3.7 K/s. The mole fraction of gold in each alloy is indicated adjacent to the corresponding spectrum.

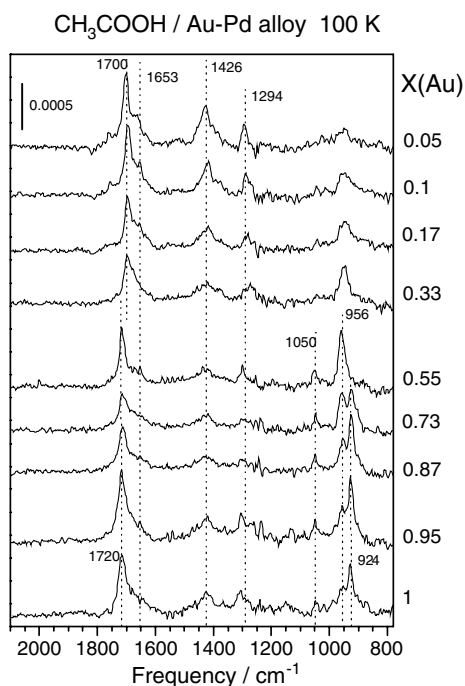


Fig. 5. RAIRS spectra collected following adsorption of acetic acid (1.2 L) on various Au/Pd(111) alloys at 100 K where the mole fraction of gold in each alloy is indicated adjacent to the corresponding spectrum.

at ~ 100 K (Fig. 5), after annealing to ~ 210 K (Fig. 6) and to ~ 240 K (Fig. 7) since the η^2 -acetate species forms at approximately this temperature on Pd(111) [1]. For the latter experiments, the sample was heated to either ~ 210 or 240 K for a period of 5 s, then allowed to cool to 100 K

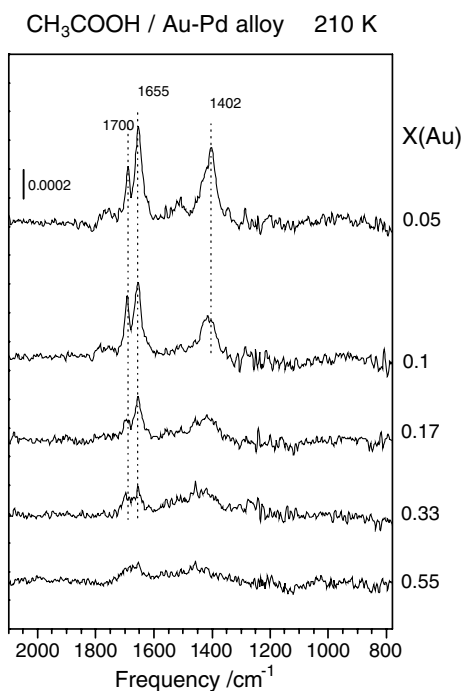


Fig. 6. RAIRS spectra collected following adsorption of acetic acid (1.2 L) on various Au/Pd(111) alloys at 100 K and annealing to 210 K for 5 s and then allowing to cool to 100 K, when the spectra were recorded. The mole fraction of gold in each alloy is indicated adjacent to the corresponding spectrum.

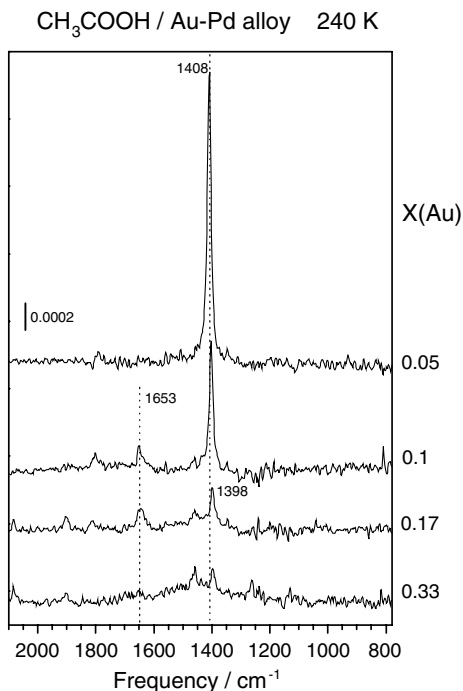


Fig. 7. RAIRS spectra collected following adsorption of acetic acid (1.2 L) on various Au/Pd(111) alloys at 100 K and annealing to 240 K for 5 s and then allowing to cool to 100 K, when the spectra were recorded. The mole fraction of gold in each alloy is indicated adjacent to the corresponding spectrum.

once again, following which the infrared spectra were collected.

Fig. 5 displays the RAIRS data for acetic acid adsorbed on various gold–palladium alloys at ~ 100 K, where the gold mole fraction, X , measured from the Auger spectrum, is displayed adjacent to the corresponding infrared spectrum. There are clearly substantial differences in the spectra as a function of alloy composition. The spectrum for the gold–palladium alloy surface with a gold mole fraction of ~ 1 exhibits features at 1720 cm^{-1} with a low-frequency tail extending to $\sim 1600\text{ cm}^{-1}$ with additional peaks at 1426 (broad), 1294 (broad), 1050 , 956 and 924 cm^{-1} . These values for the gold–palladium alloy are in reasonable agreement with those for acetic acid on the clean surface [1,19] and the assignments are summarized in Table 1. In particular, the presence of the $\gamma(\text{OH})$ mode (at ~ 924 and 956 cm^{-1}) and the fact that acetic acid desorbs molecularly for gold concentrations >0.5 (Figs. 1–4) indicates that no O–H bond scission has occurred. The persistence of features in the OH bending region for gold concentrations as low as ~ 0.55 is also in accord with the lack of CO_2 (Fig. 3) or hydrogen (Fig. 2) desorption from these surfaces and indicates that acetic acid adsorbs and desorbs molecularly for gold mole fractions ≥ 0.5 .

At a gold concentration of 0.33 , the C=O stretching frequency shifts to $\sim 1700\text{ cm}^{-1}$ again with a low-frequency tail, indicative of the presence of another species on the surface. The spectrum still include features at ~ 1426 ($\delta_s(\text{CH}_3)$) and 1294 ($\nu(\text{C}-\text{O})$) cm^{-1} , while the $\rho(\text{CH}_3)$ mode (at $\sim 1050\text{ cm}^{-1}$) is no longer present. As the gold concentration decreases further to <0.33 , the $\gamma(\text{OH})$ mode decreases in intensity while the $\delta_s(\text{CH}_3)$ ($\sim 1426\text{ cm}^{-1}$) and $\nu(\text{C}-\text{O})$ ($\sim 1294\text{ cm}^{-1}$) modes intensify, while the shoulder at $\sim 1653\text{ cm}^{-1}$ becomes more distinct.

Further clues to the nature of this surface species are provided by the data of Fig. 6, which display the spectra after annealing to ~ 210 K. This annealing temperature was selected since it is slightly above the acetic acid desorption temperature in TPD (Fig. 1). Therefore, for clarity, only those spectra for gold concentrations less than ~ 0.55 are displayed. After heating to ~ 210 K, the $\sim 1700\text{ cm}^{-1}$ mode decreases in intensity and the $\sim 1655\text{ cm}^{-1}$ mode and the feature at $\sim 1402\text{ cm}^{-1}$ grow relative to the corresponding intensities in the spectra collected at ~ 100 K (Fig. 5). Note

that these features are not due to an η^2 -acetate species, which displays an intense peak slightly above 1400 cm^{-1} [1]. This suggests that these features are due to a monodentate acetate species, where the $\sim 1655\text{ cm}^{-1}$ peak is assigned to a $\nu(\text{C}=\text{O})$ mode. This will be discussed in greater detail below, but it should be mentioned that this assignment differs from that made previously to monodentate acetate on clean Pd(111) using high-resolution electron energy loss spectroscopy (HREELS) where a feature at $\sim 1735\text{ cm}^{-1}$ was assigned to this species [1]. However, the absence of any $\gamma(\text{OH})$ modes due to acetic acid between 920 and 960 cm^{-1} implies the presence of an acetate species. Further support for this assignment comes from the spectra in Fig. 7 obtained after annealing gold–palladium alloy surface to ~ 240 K where again these are displayed for gold concentrations less than ~ 0.5 for clarity. These display an intense feature at $\sim 1400\text{ cm}^{-1}$ (between 1398 and 1408 cm^{-1} depending on gold concentration) assigned to the symmetric OCO stretching mode of the bidentate acetate [1,20]. The intensity of the $\sim 1400\text{ cm}^{-1}$ peak increases with decreasing gold content in the alloy but only starts to form for gold mole fractions less than ~ 0.33 (Fig. 7). However, the 1653 cm^{-1} feature is still (weakly) present at this higher annealing temperature for gold concentrations of 0.17 and 0.10 . The intermediate observed at ~ 210 K has predominantly evolved into an η^2 -acetate species, providing further support for the assignment of the 1653 cm^{-1} mode to an η^1 -species.

4. Discussion

The results presented above indicate the clear presence of three regimes with different acetic-acid-derived structures on Au/Pd(111) alloys depending on gold concentration. For gold concentrations above ~ 0.5 , acetic acid adsorbs and desorbs intact, while an η^1 -acetate species forms at lower concentrations and finally an η^2 -acetate species forms on heating for gold concentrations below ~ 0.17 . These conclusions are outlined in greater detail below. It should be noted that the gold concentrations presented here are derived from calibrations based on Auger measurements [10] and must therefore be viewed with

Table 1

Comparison of the vibrational frequencies of acetic acid on a Au/Pd(111) alloy with gold mole fraction of ~ 1.0 , with vibrational frequencies on clean Pd(111) and for the monomer, dimer and solid

Assignment	Vibrational frequencies (cm^{-1})					
	Au/Pd(111)	Pd(111) ^a	Pd(111) ^b	Monomer	Dimer	Solid
$\nu(\text{C}=\text{O})$	1720	1735	1685	1799	1683	1648
$\delta_s(\text{CH}_3)^*$	1426	1415	1425	1401/1340	1431/1371	1448/1356
$\nu(\text{C}-\text{O})$	1294	–	1310	1279	1255	1284
$\rho(\text{CH}_3)$	1052	–	–	–	–	–
$\gamma(\text{OH})$	923/958	960	955	1192	944	923

ν – stretch, δ – deformation, γ – bending, ρ – rocking modes.

*See discussion in text.

^a Ref. [1].

^b Ref. [19].

caution. Nevertheless, while the absolute values of the gold concentration may be in error by a small amount, the trends in the surface chemistry as a function of concentration will be correct. Note, however, as discussed above, the concentration in the outermost layer is likely to be substantially higher.

We turn our attention first to the adsorption of acetic acid on alloy surfaces with gold concentrations greater than ~ 0.5 . There is no previous work studying acetic acid on gold surfaces for comparison. Some work has been carried out, however, for formic acid on Au(110) [21] showing that it desorbs molecularly at ~ 210 K yielding an desorption activation energy of ~ 54 kJ/mol. The lack of reactivity of gold is confirmed by the observation that methanol desorbs intact from Au(110) at ~ 200 K [22] and acetone from Au(111) at ~ 160 K [23]. The lack of decomposition products over the range of gold concentration (Figs. 2–4) is consistent with these observations and indicates that the acetic acid adsorbs and desorbs intact with an activation energy of ~ 52 kJ/mol (Fig. 1), close to the value found for formic acid on gold [21].

Furthermore, the vibrational frequencies are consistent with the presence of molecular acetic acid on the surface (Fig. 5 and Table 1) where the intense $\gamma(\text{OH})$ modes confirm the presence of the intact molecule [1]. The shape of the features in this region, however, varies substantially with alloy composition. In particular, the 923 cm^{-1} feature is much more intense than that at $\sim 956\text{ cm}^{-1}$ for an alloy with a gold mole fraction of ~ 1 . Reference to Table 1 suggests that the 923 cm^{-1} mode is associated with catemers of acetic acid on the surface and these have been proposed previously on clean Pd(111) [17]. The low-frequency shoulder on the C=O stretching mode may also be due to these catemers. As the gold concentration decreases to 0.73, the intensity of the 924 cm^{-1} feature decreases substantially and this is accompanied by an increase in the intensity of the mode at 956 cm^{-1} (Fig. 5). An increase in the $\gamma(\text{OH})$ frequency suggests the formation of smaller catemers as the gold coverage increases. The presence of dimers is indicated by a $\gamma(\text{OH})$ mode at 944 cm^{-1} (Table 1), slightly lower than the value of 956 cm^{-1} observed on the surface, but this value is substantially lower than that expected for monomeric species. Thus, while it is not possible to assign these modes to the existence of a particular catemer on the surface, the results indicate that larger catemers form on the surfaces of alloys with gold concentrations greater than 0.73, while smaller catemers form on surfaces with lower gold concentrations. While various catemers are present on surfaces with gold concentrations greater than ~ 0.55 , at a concentration of ~ 0.55 only a single (perhaps dimeric) species exists. Note that HREELS studies of formic acid on Au(111) at 100 K also find formic acid dimers [24].

As the gold concentration decreases to ~ 0.33 , some hydrogen (Fig. 3) and CO_2 (Fig. 2) are found to desorb indicating that a portion of the acetic acid decomposes. In addition, substantial changes are found in the infrared spectrum (Fig. 5) where, in particular, the principle C=O

stretching mode shifts to $\sim 1700\text{ cm}^{-1}$, with a low-frequency tail. The continued presence of a $\gamma(\text{OH})$ ($\sim 956\text{ cm}^{-1}$) mode suggest the presence of molecular acetic acid on the surface at 100 K, which desorbs at ~ 210 K (Fig. 1). However, the detection of a relatively small amount of decomposition products at this gold concentration (Figs. 2 and 3), and the very weak features in infrared spectrum formed by heating this surface to ~ 210 K (Fig. 6), suggest that the majority of the acetic acid desorbs molecularly for a gold mole fraction of ~ 0.33 , with only a small proportion decomposing.

As the gold concentration decreases, the intensity of the $\gamma(\text{OH})$ mode (at $\sim 950\text{ cm}^{-1}$) decreases following adsorption at 100 K (Fig. 5) indicating a lower coverage of molecular species and this effect is accompanied by the growth of features at ~ 1653 and $\sim 1426\text{ cm}^{-1}$ (Fig. 5). Heating these surfaces to ~ 210 K (Fig. 6) reduces the intensity of the $\sim 1700\text{ cm}^{-1}$ mode and results in further growth of the ~ 1653 and 1426 cm^{-1} modes, and the formation of a small amount of η^2 -acetate species is evidenced by the presence of a small peak at $\sim 1402\text{ cm}^{-1}$ on top of the broad $\sim 1426\text{ cm}^{-1}$ profile for a gold concentration of 5% (Fig. 6). The decrease in intensity of the 1700 cm^{-1} feature as well as the disappearance of the $\gamma(\text{OH})$ mode (956 cm^{-1}) are due to molecular acetic acid desorption at ~ 230 K on these alloy surfaces (Fig. 1), which does not result in the complete removal of acetic acid at ~ 210 K. The remaining features at ~ 1653 and $\sim 1420\text{ cm}^{-1}$ formed by heating to ~ 210 K (Fig. 6) for gold concentrations < 0.33 are therefore assigned to an η^1 -acetate species formed on the surface. The $\sim 1653\text{ cm}^{-1}$ peak is assigned to the asymmetric OCO stretching mode, and a geometry in which the η^1 -acetate is adsorbed onto a Pd(111) surface via a C—O—Pd bond would lead to a strong absorption by this mode in RAIRS [25]. The corresponding symmetric OCO stretching mode (which is the most intense for the η^2 -acetate and appears at $\sim 1400\text{ cm}^{-1}$ [1,20]) will be weak for an η^1 -acetate species. As noted in Table 1, the $\sim 1426\text{ cm}^{-1}$ mode has been assigned to $\delta_s(\text{CH}_3)$ [26,27] and in the η^1 -acetate, the C—C bond of the methyl group would be oriented close to parallel to the surface. However, a mode at $\sim 1426\text{ cm}^{-1}$ is more likely to be due to an asymmetric methyl deformation ($\delta_a(\text{CH}_3)$), which would become intense in the η^1 -acetate geometry. This result indicates that the activation energy for the formation of the η^1 -acetate species on alloy surfaces containing between $\sim 17\%$ and 5% gold is close to that for acetic acid desorption (~ 50 kJ/mol) since it forms over the temperature range at which acetic acid desorbs from the surface (~ 210 K, Fig. 6).

The η^1 -acetate species is relatively unstable and either forms bidentate acetate or thermally decomposes by heating to ~ 240 K (Fig. 7). Some low-temperature (~ 280 K) hydrogen desorption is detected for gold concentrations less than ~ 0.5 (Fig. 3) and this may be due to the hydrogen removed from the acetic acid to form the η^1 -acetate or to the decomposition of the η^1 -acetate itself, since this desorbs at close to the temperature at which hydrogen desorbs

from Pd(111) [28,29] indicating that it is desorption rather than decomposition-rate limited. The coverage of η^1 -species remaining on the surface at ~ 240 K is very low (Fig. 7), and the only species stable at this temperature is the bidentate acetate species indicated by the sharp feature at ~ 1402 cm^{-1} . Thus, the hydrogen (Fig. 2), CO_2 (Fig. 4) and CO (Fig. 4) desorption at higher temperatures in these cases is assigned to bidentate acetate decomposition. The first species to desorb from the surface at these low gold concentrations is hydrogen where the hydrogen desorption peak shifts to higher temperatures as the gold concentration decreases, from ~ 320 K for a gold mole fraction of ~ 0.17 to ~ 350 K for a value of ~ 0.03 , suggesting that the presence of even a small amount of gold destabilizes the bidentate acetate species. Since this is proposed to be the acetic-acid-derived reactant in the catalytic synthesis of VAM [8], this is likely to have profound effects on the catalytic activity of the alloy.

The observation that η^1 -species only form for gold concentrations lower than ~ 0.5 and that the η^2 -species forms at gold concentrations lower than ~ 0.17 suggests that their formation is not only limited by the availability of surface palladium sites but also implies that there is a strong electronic modification of the activity of palladium. For example, there are a large number of isolated palladium sites, and even a reasonable number of bridge sites on a Au/Pd(111) alloy surface to accommodate η^1 -species, for gold concentrations above 0.5, while only molecular species are found. Likewise, η^2 -species, where the oxygen bonds to two adjacent atop sites on Pd(111) [2] only form when the palladium concentration exceeds ~ 0.83 , while there would be expected to be a substantial proportion of bridge sites available on the surface at much lower palladium concentrations. However, these correlations should, at this stage, be viewed with caution since the surface layer is likely to be enriched with gold compared to the composition of the near surface region [16].

5. Conclusions

Acetic acid adsorbs molecularly on a Au/Pd(111) alloy surface for gold concentrations in the alloy greater than ~ 0.33 . The acetic acid desorbs with an activation energy of ~ 50 kJ/mol and forms catemers on the surface, particularly when the gold concentration is large. When the gold concentration is less than ~ 0.33 , adsorption of acetic acid at 80 K and heating to ~ 210 K forms η^1 -acetate species on the surface. On further heating, these can either ther-

mally decompose to eventually evolve hydrogen, water and oxides of carbon, or form η^2 -acetate species, where the coverage of reactively formed η^2 -acetate species increases with decreasing gold concentration.

Acknowledgement

We gratefully acknowledge support of this work by the US Department of Energy, Division of Chemical Sciences, Office of Basic Energy Sciences, under Grant Number DE-FG02-92ER14289.

References

- [1] R.D. Haley, M.S. Tikhov, R.M. Lambert, *Catal. Lett.* 76 (2001) 125.
- [2] J. James, D.K. Saldin, T. Zheng, W.T. Tysoe, D.S. Sholl, *Catal. Today*, 105 (2005) 74.
- [3] E. Hansen, M. Neurock, *J. Phys. Chem. B* 105 (2001) 9218.
- [4] M. Neurock, *J. Catal.* 216 (2003) 73.
- [5] M. Bowker, C. Morgan, J. Couves, *Surf. Sci.* 555 (2004) 145.
- [6] J.L. Davis, M. Barteau, *Surf. Sci.* 256 (1991) 50.
- [7] B. Samanos, P. Boutry, R. Montarnal, *J. Catal.* 23 (1971) 19.
- [8] D. Stacchiola, F. Calaza, L. Burkholder, A.W. Schwabacher, M. Neurock, W.T. Tysoe, *Angew. Chem., Int. Ed.* 44 (2005) 4572.
- [9] *Cat. Gold News*, Issue 4 (spring 2003).
- [10] C.J. Baddeley, M. Tikhov, C. Hardacre, J.R. Lomas, R.M. Lambert, *J. Phys. Chem.* 100 (1996) 2189.
- [11] M. Kaltchev, A.W. Thompson, W.T. Tysoe, *Surf. Sci.* 391 (1997) 145.
- [12] D. Stacchiola, L. Burkholder, W.T. Tysoe, *Surf. Sci.* 511 (2002) 215.
- [13] W.J. Wytenburg, R.M. Lambert, *J. Vac. Sci. Technol. A* 10 (1992) 3597.
- [14] L.Z. Mezey, J. Giber, *Jpn. J. Appl. Phys.* 11 (1982) 1569.
- [15] W.R. Tyson, W.A. Miller, *Surf. Sci.* 62 (1977) 267.
- [16] C.W. Yi, K. Luo, T. Wei, D.W. Goodman, *J. Phys. Chem. B* 109 (2005) 8535.
- [17] F. Calaza, F. Gao, Z. Li, W.T. Tysoe, *Surf. Sci.*, in press, doi:10.1016/j.susc.2006.10.039.
- [18] P.A. Redhead, *Vacuum* 12 (1962) 203.
- [19] J.L. Davis, M.A. Barteau, *Langmuir* 5 (1989) 1299.
- [20] D. Stacchiola, F. Calaza, L. Burkholder, W.T. Tysoe, *J. Am. Chem. Soc.* 126 (2004) 15384.
- [21] D.A. Outka, R.J. Madix, *Surf. Sci.* 179 (1987) 361.
- [22] D.A. Outka, R.J. Madix, *J. Am. Chem. Soc.* 109 (1987) 1708.
- [23] D. Syomin, B.E. Koel, *Surf. Sci.* 498 (2002) 53.
- [24] M. Chtaib, P.A. Thiry, J.J. Pireaux, J.P. Delrue, R. Caudano, *Surf. Sci.* 162 (1985) 245.
- [25] R.G. Greenler, *J. Chem. Phys.* 44 (1966) 310.
- [26] P.F. Krause, J.E. Katon, J.M. Rodgers, D.B. Phillips, *Appl. Spectrosc.* 31 (1997) 110.
- [27] W. Weltner Jr., *J. Am. Chem. Soc.* 77 (1995) 3941.
- [28] D. Stacchiola, L. Burkholder, W.T. Tysoe, *Surf. Sci.* 542 (2003) 129.
- [29] L. Burkholder, D. Stacchiola, W.T. Tysoe, *Surf. Rev. Lett.* 10 (2003) 909.